Chemosphere 74 (2009) 804–809

Contents lists available at ScienceDirect

Chemosphere

journal homepage: www.elsevier.com/locate/chemosphere

Kinetics of the chemical reduction of nitrate by zero-valent iron

J.M. Rodríguez-Maroto *, F. García-Herruzo, A. García-Rubio, C. Gómez-Lahoz, C. Vereda-Alonso

Department of Chemical Engineering, University of Malaga, 29071 Malaga, Spain

ARTICLE INFO

Article history:
Received 17 July 2008
Received in revised form 15 October 2008
Accepted 15 October 2008
Available online 28 November 2008

Keywords:
Reduction nitrate
Zero-valent iron
Permeable reactive barrier
Eley–Rideal kinetics

ABSTRACT

The use of reactive barriers is one of the preferred remediation technologies for the remediation of groundwater contamination. An adequate design of these barriers requires the understanding of the kinetics of the reaction between the target contaminant and the solid phase in the barrier. A study of the kinetics between metallic iron and aqueous nitrate is presented in this paper. Published literature regarding this reaction indicates that researchers are far from a consensus about the mechanism of this reaction. This paper presents the results obtained from experiments performed at different constant pH values and iron dosages, together with a mathematical analysis of the kinetic results. We have found that an Eley–Rideal kinetic model yields a good explanation of the relatively complicated dependence between rate of nitrate reduction and the pH value of the solution.

1. Introduction

Nitrate contamination has become a major water quality problem in agricultural regions. A high nitrate level in surface waters poses a serious threat to aquatic ecosystems due to the increase of algae growth, which usually leads to a decrease of the biodiversity (eutrophication problem). High nitrate concentration in drinking water presents a risk to the human health. Nitrate itself is relatively non-toxic; however, it can be reduced to nitrite, which combines with hemoglobin in the blood to form methemoglobin. Methemoglobinemia occurs mostly in children and is also known as "blue-baby syndrome" (Shuval and Gruener, 1977; Kapoor and Viraraghavan, 1997). There is also circumstantial evidence linking ingestion of nitrate to gastric cancer and birth defects. Consequently, the concentration of nitrate and nitrite in drinking water has been regulated. The levels in drinking water of nitrate and nitrite established by the European Union legislation (Council Directive 91/676/EEC) are 50 and 0.5 mg L^{-1}, respectively. In the United States, EPA establishes the maximum contaminant levels of 10 mg NO_3^-–N L^{-1} and 1 mg NO_2^-–N L^{-1} for drinking water (EPA, 2003).

Nitrate-contaminated waters are commonly treated by ion exchange or reverse osmosis. However, these traditional treatments are relatively expensive, because they require frequent regeneration of the media, or generate secondary brine wastes that may pose a disposal problem. Biological denitrification is another alternative to remove nitrate from water (Kim et al., 2003; Davis, 2007), because the microbial process reduces the nitrate to innocuous nitrogen gas rather than ammonium and generally results in lower operating costs as compared to ion exchange or reverse osmosis. However, this process can produce excessive biomass and soluble microbial products that require further treatment of the denitrified water (aeration and disinfection). Moreover, the denitrification process is generally slow and sometimes incomplete as compared to chemical reduction.

In recent years, the success of iron metal in treating groundwater containing chlorinated solvents has stimulated a significant interest in the application of zero-valent iron (Fe^0) to other contaminants such as chromium(VI), nitrate and nitrite, thus emerging as a novel chemical process for the use of in situ reactive barrier intercepting and treating groundwater plumes containing these contaminants (Rocca et al., 2006).

It is well known that the kinetics of nitrate reduction by Fe^0 in an anoxic aqueous phase is strongly dependent on the proton concentration (Cheng et al., 1997; Huang et al., 1998; Zawaideh and Zhang, 1998; Alowitz and Scherer, 2002; Huang and Zhang, 2004). The study of this influence has been attained performing experiments at several constant pH values. Different experimental systems have been used to control the pH throughout the nitrate reduction. The published results indicate that experimental systems with pH controlled by the controlled addition of acid solutions have shown more reliability than the buffered systems. In the latter, the specific buffer used to control pH has shown a significant effect on the amount of nitrate reduced and poor ability to control pH throughout the experiment (Zawaideh and Zhang, 1998; Choe et al., 2000; Alowitz and Scherer, 2002; Su and Puls, 2007). However, regardless of the Fe^0 type, a rapid reduction of nitrate mainly occurs at pH values below 4 or 5 (Huang et al., 1998; Huang and Zhang, 2004).

* Corresponding author. Tel.: +34 952 131 915; fax: +34 952 132 000.
E-mail address: maroto@uma.es (J.M. Rodríguez-Maroto).

0045-6535/$ - see front matter © 2008 Elsevier Ltd. All rights reserved.
doi:10.1016/j.chemosphere.2008.10.020

The works mentioned above reveal no consensus on the mechanism of the reaction. Nevertheless, the researches performed in recent years indicate that the reducing agent could be Fe^0 coated with Fe(II)/Fe(III) oxides, with special influence of the Fe(II) component in the NO_3^- reduction to NH_4^+ (Huang and Zhang, 2004; Mishra and Farrell, 2005). Most of the reviewed works indicate NH_4^+ as the end product of nitrate reduction, although some authors suggest, without providing evidence, that when the size of the iron grains is on the nanometer scale the product is N_2 gas (Choe et al., 2000; Yang and Lee, 2005). Nevertheless, Sohn et al. (2006) have observed NH_4^+ as the main end product with nanometer scale Fe^0. Different end-product distributions have also been observed in the degradation of chlorinated compounds by different types of commercial irons (Tamara and Butler, 2004).

A wide variety of kinetic models for nitrate reduction by Fe^0 have been published: from those using a first order kinetic model with respect nitrate concentration (Cheng et al., 1997; Choe et al., 2000; Alowitz and Scherer, 2002; Choe et al., 2004), to those with apparent higher reaction order (Huang et al., 1998) or lower one (Yang and Lee, 2005). Finally, there are shifting order models corresponding to mechanisms similar to those of Langmuir (Huang and Zhang, 2004) or of Michaelis–Menten (Choe et al., 2000). The proposed kinetic expressions usually include a first order dependence on Fe^0 surface area concentration. Unfortunately, only a few of these kinetic data have been obtained in experiments with successful pH-control.

This study examines the applicability and limitations of granular Fe^0 for the chemical reduction of nitrate in aqueous solution. Specifically, we followed the kinetics of nitrate removal at different controlled pH values, with different concentration/dosage of Fe^0 and at constant temperature.

2. Experimental method

2.1. Chemicals

Sodium nitrate (99.5%) (from Carlo Erba, RPE) and a commercial fine granulated Fe^0 (Panreac, PRS) were used as received. The mean value of the diameter of these particles (0.42 mm) was obtained by sieving while their BET area was not large enough to be measured by a Micromeritics ASAP 2020 accelerated surface area analyzer. All solutions were prepared using milli-Q water (18.2 MΩ cm) from a Millipore-15Q plus system.

2.2. Experimental system

Basically it consists of a 5 L glass batch reactor with the initial NO_3^- solution that is continuously deoxygenated by N_2 bubbling which, together with a mechanical agitator, provides agitation. The temperature was regulated at 15 ± 1 °C by immersion in a thermostatic water bath. The pH value and the redox potential are periodically registered by means of Hamilton pH- and ORP- electrodes, each one connected to a pH-control system of our own manufacture. PVC tubes, which also act as baffles that improve mixing, protect these electrodes. These tubes are fitted to the openings of the reactor stopper by permeable foam, providing a secure exit for N_2 while preventing the entrance of O_2. The pH-control system consists of a graduated 100 mL burette that makes available the necessary volume of sulfuric acid solution to the reactor when the pH increases above a target pH-value. The acid volume added is controlled by an electrovalve assembled on the top of the burette. When the electrovalve is open, air comes into the burette and the acid solution drops into the reactor. This electrovalve is electronically controlled by a computer, which allows the maintenance of the pH value in the reactor within a 2% variation of the target value. The acid consumption was followed during the reaction.

2.3. Experimental procedure

About 5 L of $NaNO_3$ solution (500 mg $NO_3^- L^{-1}$), with the required amount of sulfuric acid to yield the desired pH value, is added to the thermostatic glass reactor. While the temperature of this solution is stabilized, N_2 is continuously bubbling, the mechanical agitation is activated and the pH value and redox potential recording is started. After this stabilization, the necessary amount of Fe^0 was provided.Two samples of 10 mL were withdrawn at selected times using a plastic syringe. The aqueous concentrations of NO_3^- are determined by potentiometric standard methods (US-EPA method 9210) (EPA, 2004) using an ion selective electrode (ISE) Cole Parmer 27502-30 connected to a Teknokroma pH-meter, model 555. The aqueous concentrations of NH_4^+ were also determined using an ion selective electrode (Cole Parmer 27502–03). The aqueous iron concentrations were also determined by flame atomic absorption spectroscopy (Varian AA210). About 20 duplicate samples were withdrawn by the end of the assay, less than 8% of volume of reactor. Similarly, the maximum volume of H_2SO_4 solution added for pH control throughout each assay was between 50 and 150 mL. Therefore, the opposite effects of these volume changes on the assay results are considered negligible.

In order to study the effect of pH on the kinetics of nitrate reduction, six triplicated experiments were performed at different pH values ranging from 1.5 to 4, using in each one the adequate concentration of sulfuric acid solutions for the pH-control system. The effect of the Fe^0 surface area concentration was studied in a set of duplicated experiments performed at a constant pH value of 2 and at concentrations/dosages of Fe^0 ranging from 1.2 to 24 g L^{-1}.

3. Results

As an example, Fig. 1 shows the results obtained at pH 2, 15° C and an iron dosage of 6 g L^{-1}. This represents a 333% excess of the amount required for a complete reduction of NO_3^- following Eq. (1)

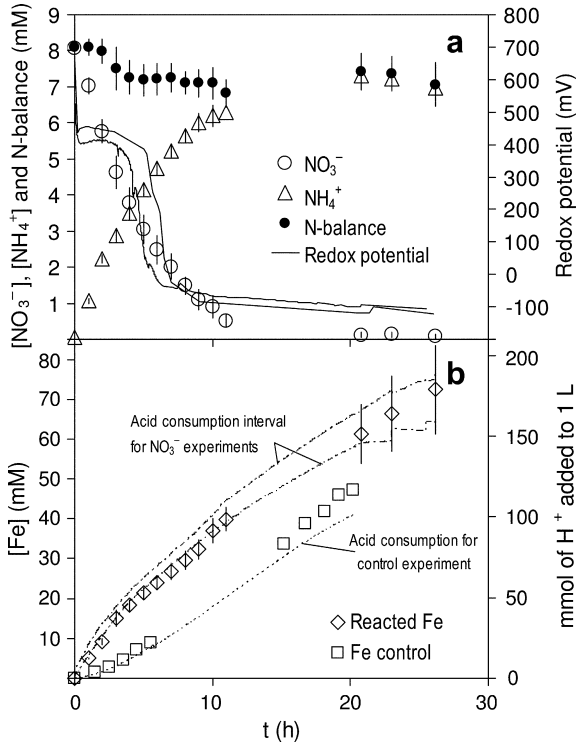

Fig. 1. Experimental results for fixed pH 2.00 ± 0.04 and iron dosage = 6 g L^{-1}.

$$4Fe^0 + NO_3^- + 10H^+ \rightarrow 4Fe^{2+} + NH_4^+ + 3H_2O \quad (1)$$

As can be seen, nitrates were almost completely transformed into ammonium in about 24 h. The nitrogen recovery was about 90% at the end of all the experiments, the losses probably due to errors in the determination of ammonium concentration. It is also possible that some nitrogen initially present as NO_3^- ends as a product different from NH_4^+. We have checked every sample for NO_2^- absence by the 8507 US EPA method using a Hach Odyssey spectrophotometer.

As can be seen, the system evolves from oxidizing conditions at the beginning (around 650 mV before Fe^0 addition and 430 mV a few minutes later) to reducing conditions (–100 mV). Fig. 1b shows the dissolved iron concentration and the acid added to maintain the pH value shown as the average of the replicate assays plus and minus the standard deviation. Note that acid consumption scale axis is 2.5 times the iron concentration one. The slope of the proton consumption curve is therefore about 2.5 times that of iron concentration although this ratio gradually decreases towards 2 at the end of the experiment. All this, together with the still significant proton consumption rate when almost all nitrates are reduced, indicate that some other proton sink different to the nitrate reduction to ammonium Eq. (1) is present. Among the possible reactions that could be taking place is the following competitive oxidation of Fe^0

$$Fe^0 + 2H^+ \rightarrow Fe^{2+} + H_2 \quad (2)$$

A control test without nitrate was performed in order to investigate the rate of iron oxidation and proton consumption. As can be seen in Fig. 1b, this control test presents a rather constant rate of proton demand which is quite similar to the one observed at the end of the nitrate reduction experiment, so the reaction given by Eq. (2) should be considered together with nitrate reduction.

Fig. 2 shows the nitrate concentration against the reaction time at different fixed pH values. As can be seen, the kinetics of reduction of nitrates strongly depends on the protons concentration. Total reduction of nitrate is obtained in a few hours for pH values below 2.5, whereas only about 37% of nitrate is reduced after 22 d in the assays performed at pH of 4. On the other hand, the experiments performed at different Fe^0 dosages indicate that the rate of nitrate reduction increases with the metal surface concentration, as can be expected.

4. Discussion

4.1. Kinetic model

In a first attempt, we have explored the nitrate reduction kinetics using an empirical rate equation of *n*th order. The solid lines shown in Fig. 2 correspond to the best fit for this kind of equation and the legend shows the value obtained for *n*. As can be seen, the changes observed in the order of reaction are difficult to be explained as a consequence of the different constant pH values. Therefore, the kinetic model to be proposed should somehow explain these variations on the order of reaction that have been also previously observed in the literature (Yang and Lee, 2005).

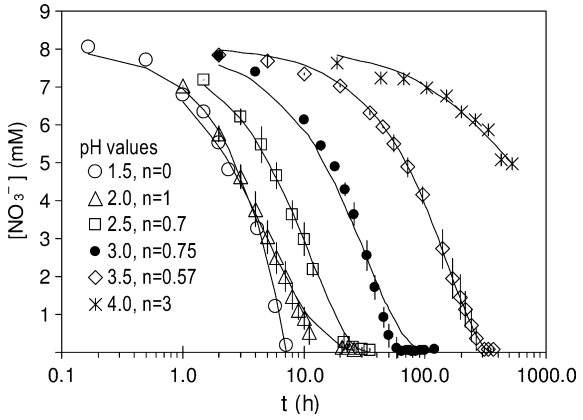

Fig. 2. Experimental NO_3^- removal for pH values between 1.5 and 4.0 and iron dosage of 6 g L^{-1}.

Furtheremore, we have found that a shift in the reaction order can be observed as the concentration of nitrates decreases. This kind of behaviour is usually described using models for the kinetics of surface-catalyzed gas reactions such as Langmuir–Hinshelwood or Eley–Rideal mechanisms (Steinfeld et al, 1989; Elnashaie and Elshishini, 1993). We have obtained best results with the Eley–Rideal mechanism, in which the reduction reaction step on the iron surface (single-site) controls the overall process. In other words, the reactants adsorption and the products desorption are very fast as compared with the reaction step, and therefore adsorption–desorption equilibrium can be assumed. The model proposes a competitive adsorption for both nitrates and protons on the active-site on the iron surface. Before these adsorptions, the active site would have retained a proton. The kinetic and equilibrium expressions are shown below, where θ_i represents the fraction of the active-site covered by the *i*th species and θ_S the fraction of active-site uncovered:

– Proton adsorption on the active site (S)

$$H^+ + S \underset{k_{-0}}{\overset{k_0}{\rightleftarrows}} (S\cdot H^+)_{ads}, \qquad r_0 = k_0[H^+]\theta_s - k_{-0}\theta_{SH} \quad (3)$$

– Nitrate adsorption on the active site (S) after the proton adsorption

$$NO_3^- + (S\cdot H^+)_{ads} \underset{k_{-1}}{\overset{k_1}{\rightleftarrows}} (S\cdot H^+\cdot NO_3^-)_{ads},$$
$$r_1 = k_1[NO_3^-]\theta_{SH} - k_{-1}\theta_N \quad (4)$$

– Second proton adsorption on the active site (S)

$$H^+ + (S\cdot H^+)_{ads} \underset{k_{-2}}{\overset{k_2}{\rightleftarrows}} (S\cdot H^+\cdot H^+)_{ads}, \quad r_2 = k_2[H^+]\theta_{SH} - k_{-2}\theta_H \quad (5)$$

– Reduction of the adsorpted nitrates, $(S\cdot H^+\cdot NO_3^-)_{ads}$, considering irreversible reaction with a fast desorption of the reaction products. In this case, the reduction of nitrate follows two different paths simultaneously. The first one produces Fe^{2+} and the other one produces FeO

$$(S\cdot H^+\cdot NO_3^-)_{ads} + 4Fe^0(s) + 9H^+ \overset{k_3}{\rightarrow} 4Fe^{2+} + NH_4^+ + S + 3H_2O, \quad r_3 = k_3\theta_N[H^+] \quad (6)$$

$$(S\cdot H^+\cdot NO_3^-)_{ads} + 4Fe^0(s) + H^+ + H_2O \overset{k_4}{\rightarrow} 4FeO(s) + NH_4^+ + S, \quad r_4 = k_4\theta_N[H^+] \quad (7)$$

– Reduction of adsorpted protons, considering irreversible reaction with fast desorption of the reaction products

$$(S\cdot H^+\cdot H^+)_{ads} + Fe^0(s) \overset{k_5}{\rightarrow} Fe^{2+} + H_2(g) + S, \quad r_5 = k_5\theta_H \quad (8)$$

Assuming that the adsorption of both nitrate and protons on the active sites is fast enough to consider that equilibrium is achieved in 3–5 and taking into account that $\theta_S + \theta_{SH} + \theta_N + \theta_H = 1$, then the fraction of active-site covered by nitrates and protons can be expressed as a function of their adsorption equilibrium constants (K_0, K_1 and K_2) and their aqueous concentration, this is

$$K_0 = \frac{k_0}{k_{-0}} = \frac{\theta_{SH}}{[H^+]\theta_S},\ K_1 = \frac{k_1}{k_{-1}} = \frac{\theta_N}{[NO_3^-]\theta_{SH}},\ K_2 = \frac{k_2}{k_{-2}}\frac{\theta_H}{[H^+]\theta_{SH}} \quad (9)$$

$$\theta_N = \frac{K_0K_1[NO_3^-][H^+]}{1 + K_0[H^+] + K_0K_2[H^+]^2 + K_0K_1[NO_3^-][H^+]}$$

$$\theta_H = \frac{K_0K_2[H^+]^2}{1 + K_0[H^+] + K_0K_2[H^+]^2 + K_0K_1[NO_3^-][H^+]} \quad (10)$$

And therefore, the rate expressions of the rate determining steps 6–8 are

$$r_3 = k_3[H^+]\frac{K_0K_1[NO_3^-][H^+]}{1+K_0[H^+]+K_0K_2[H^+]^2+K_0K_1[NO_3^-][H^+]} = \frac{k_3[H^+][NO_3^-]}{\frac{1}{K_0K_1[H^+]}+\frac{1}{K_1}+\frac{K_2[H^+]}{K_1}+[NO_3^-]} \quad (11)$$

$$r_4 = k_4[H^+]\frac{K_0K_1[NO_3^-][H^+]}{1+K_0[H^+]+K_0K_2[H^+]^2+K_0K_1[NO_3^-][H^+]} = \frac{k_4[H^+][NO_3^-]}{\frac{1}{K_0K_1[H^+]}+\frac{1}{K_1}+\frac{K_2[H^+]}{K_1}+[NO_3^-]} \quad (12)$$

$$r_5 = k_5\frac{K_0K_2[H^+]^2}{1+K_0[H^+]+K_0K_2[H^+]^2+K_0K_1[NO_3^-][H^+]} = \frac{\frac{k_5K_2}{K_1}[H^+]}{\frac{1}{K_0K_1[H^+]}+\frac{1}{K_1}+\frac{K_2[H^+]}{K_1}+[NO_3^-]} \quad (13)$$

As can be seen in these last three equations, when the reduction is performed at a constant pH value, r_3, r_4 and r_5 only depend on the nitrate concentration. The rate of nitrate reduction will be expressed as

$$-\frac{d[NO_3^-]}{dt} = r_3 + r_4 = (k_3 + k_4)\frac{[H^+][NO_3^-]}{\frac{1}{K_0K_1[H^+]}+\frac{1}{K_1}+\frac{K_2[H^+]}{K_1}+[NO_3^-]} = \frac{f_1[NO_3^-]}{f_2+[NO_3^-]} \quad (14)$$

where

$$f_1 = (k_3 + k_4)[H^+] \text{ and } f_2 = \frac{1}{K_0K_1[H^+]} + \frac{1}{K_1} + \frac{K_2[H^+]}{K_1} \quad (15)$$

The rate of iron oxidation to Fe^{2+} is given by the sum of both rate-determining steps

$$\frac{d[Fe^{+2}]}{dt} = 4r_3 + r_5 = \frac{4k_3[H^+][NO_3^-] + \frac{k_5K_2}{K_1}[H^+]}{\frac{1}{K_0K_1[H^+]}+\frac{1}{K_1}+\frac{K_2[H^+]}{K_1}+[NO_3^-]} = \frac{4f_3[NO_3^-]+f_5}{f_2+[NO_3^-]} \quad (16)$$

$$\text{where } f_3 = k_3[H^+] \text{ and} f_5 = \frac{k_5K_2}{K_1}[H^+] \quad (17)$$

And finally, the rate of proton consumption is

$$-\frac{d[H^+]}{dt} = 10r_3 + 2r_4 + 2r_5 = \frac{10k_3[H^+][NO_3^-] + 2k_4[H^+][NO_3^-] + 2\frac{k_5K_2}{K_1}[H^+]}{\frac{1}{K_0K_1[H^+]}+\frac{1}{K_1}+\frac{K_2[H^+]}{K_1}+[NO_3^-]} = \frac{10f_3[NO_3^-]+2f_4[NO_3^-]+2f_5}{f_2+[NO_3^-]} \quad (18)$$

where $f_4 = k_4[H^+]$.

4.2. Kinetic model application

The procedure followed to fit the kinetic model to the experimental data at each constant pH value is as follows: first, the least squares fitting of the experimental nitrate concentration evolution to the kinetic expression of nitrate reduction (14) provides the values of f_1 and f_2. Second, in a similar way, the least squares fitting of the experimental iron concentration evolution to the kinetic expression for Fe^{2+} (16) yields the values of f_3 and f_5; it should be noted that the values of f_2 are already known from the first step. Third, the values of f_4 at each pH value are obtained from f_1 and f_3 ($f_4 = f_1 - f_3$). Then, the calculation procedure is checked by the

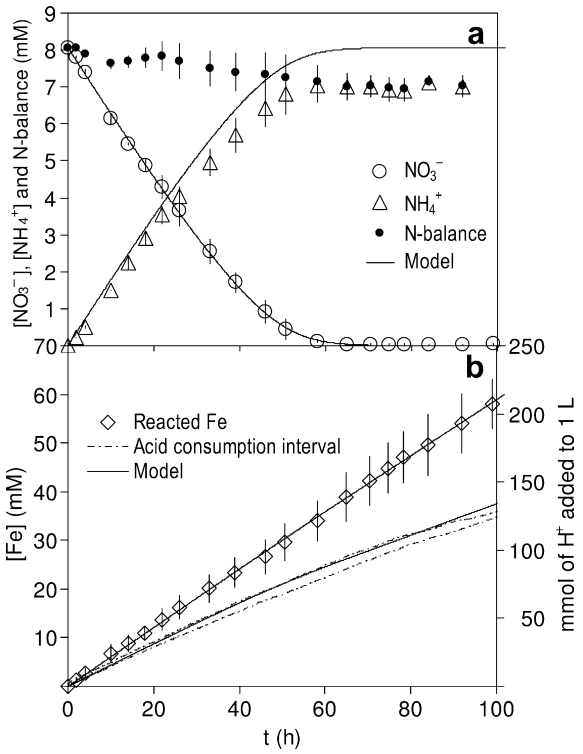

Fig. 3. Experimental and model results for pH 3.

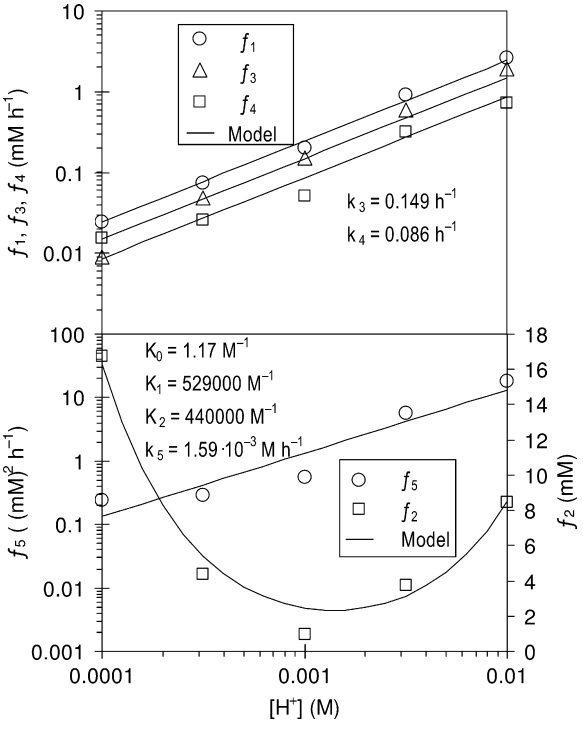

Fig. 4. Fitting of the f_i parameters to the model expressions.

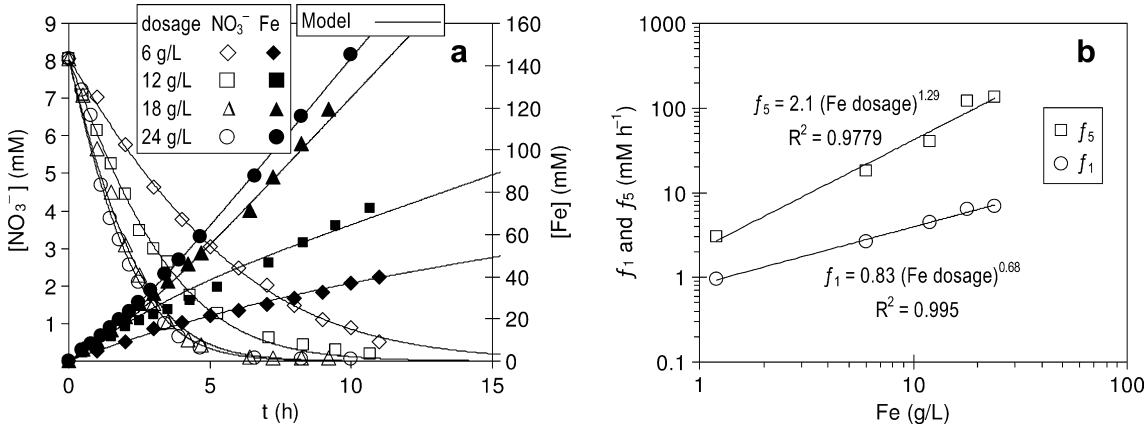

Fig. 5. Experimental and model results for nitrate and iron concentration evolutions at different iron dosage and a fixed pH value of 2.

comparison between the experimental and the model results for proton consumption (18) using the parameter values already obtained.

4.3. Influence of the pH value

As an example, Fig. 3 shows the model and experimental results for pH = 3.0. In Fig. 3a the concentrations of nitrate and ammonia and the nitrogen balance are represented against the reaction time. As indicated in the Section 3, the determination of ammonium concentration by ISE presents errors that can be close to 10%, therefore the fittings were performed for the experimental nitrate concentration using f_1 and f_2 as fitting parameters. Similar results were obtained for the other pH values explored, with determination coefficient values between $R^2 = 0.9985$ and 0.9997. It should be noted that the nitrogen balance differences present similar values in all the experiments and depend on the ammonium concentration more than on the reaction time.

Fig. 3b shows the results for Fe^{2+} concentration and acid consumption evolution. As explained above, the model results are obtained using the values of f_1 and f_2 obtained from the nitrate data fitting, and using f_3 and f_5 as fitting parameters. Again good determination coefficient values (from $R^2 = 0.9929$ to 0.9985) were obtained for all the six pH values explored. The determination coefficient values for the non-fitted acid consumption were between 0.9385 and 0.9927. This gives an important reliability on the model.

The values of the kinetic and equilibrium coefficients of the model can now be obtained from the values of f_i at the different pH values essayed. Except for f_2, the logarithm of the parameter values was used to obtain the best fit. The values of the parameters f_i against the pH value together with the model results are shown in Fig. 4. The results corresponding to pH 1.5 are not consistent with the trend observed for the other pH values. This observation is probably due to the arising of mass transfer limitations when the chemical reaction becomes very fast. This is also consistent with the fact that the results obtained for pH values of 1.5 and 2.0 are quite similar, as can be seen in Fig. 2. Therefore, results for pH 1.5 are omitted in the following figures and calculations.

As indicated in the introduction section the wide variation of the order of reaction with respect to the nitrate concentration reported previously is difficult to explain. As far as the authors know, only the work of Huang and Zhang (2004) presented a kinetic equation with shifting order of reaction by means of a Langmuir kinetic equation. The equivalent value to their specific nitrate reduction rate ($0.200\ L\ m^{-2}\ min^{-1}$) can be calculated from our model results as $0.256\ L\ m^{-2}\ min^{-1}$ after normalizing our parameter values with respect to the surface concentration. Since the specific surface is not large enough to be measured directly, we have calculated the specific surface, assuming spherical shape for the Fe particles after classification by sieving, as 2.6×10^{-3} ($m^2\ g^{-1}$). Nevertheless, Huang and Zhang model is unable to explain our observation that the variation of f_2 with respect to the pH value Eq. (15) presents a minimum, while their analogous term (K'_N) increases continuously with the proton concentration.

4.4. Influence of the Fe^0 dosage

As expected, the surface area concentration of Fe^0 strongly influences the kinetics of nitrate reduction, indicating that this reaction should be taking place at the metal surface. Fig. 5 presents the model and experimental results at a fixed pH value of 2 and different iron dosages (1.2–24 g $Fe^0\ L^{-1}$). Since f_2 is only related to thermodynamic parameters Eq. (15) the experimental nitrate concentration evolution was performed using only f_1 as fitting parameter while the value for f_2 was the one obtained in the *influence of the pH value* paragraph. The values of the remaining parameters were obtained following the same procedure described in the kinetic model application paragraph. As can be seen, good fitting is obtained for both experimental concentration evolutions at each iron dosage. Although not shown the model adequately reproduces the experimental acid consumption too.

The values of the parameters f_1 and f_5 obtained are represented against the iron dosage in Fig. 5b. As indicated in the kinetic model paragraph, f_1 is related to the reduction of the adsorpted nitrates whereas f_5 is related to reduction of the adsorpted protons. The influence of the iron surface concentration is analyzed by fitting these two parameters to a potential function on the iron dosage, so the exponent indicates the apparent reaction order with respect to the iron surface concentration for both reduction reactions.

The apparent reaction order with respect to the iron surface concentration is close to 2/3 for the reduction of adsorpted nitrate. This value is typical (Levenspiel, 1999) when the chemical reaction rate is the rate-limiting step in the solid–fluid reaction models where the solid particles are considered spherical. Nevertheless, in the reduction of adsorpted protons, the apparent reaction order almost doubled the 2/3 coefficient, that may indicate that two active sites on the iron surface are involved on the mechanism described by Eq. (8).

Acknowledgement

C. Gómez-Lahoz and C. Vereda-Alonso acknowledge the economic support from the Secretaría General de Universidades,

Investigación y Tecnología, of the Junta de Andalucía (Spain), through the Program "Medidas de Impulso de la Sociedad del Conocimiento en Andalucia".

References

Alowitz, M.J., Scherer, M.M., 2002. Kinetics of nitrate, nitrite and Cr(VI) reduction by iron metal. Environ. Sci. Technol. 36, 299–306.

Cheng, F., Muftikian, R., Fernando, Q., Korte, N., 1997. Reduction of nitrate to ammonia by zero-valent iron. Chemosphere 35, 2689–2695.

Choe, S., Chang, Y., Hwang, K., Khim, J., 2000. Kinetics of reductive denitrification by nanoscale zero-valent iron. Chemosphere 41, 1307–1311.

Choe, S., Liljestrand, H.M., Kim, J., 2004. Nitrate reduction by zero-valent iron under different pH regimes. Appl. Geochem. 19, 335–342.

Council Directive 91/676/EEC. Official Journal L 375, 31/12/1991, pp. 0001–0008.

Davis, A.P., 2007. Field performance of bioretention: water quality. Environ. Eng. Sci. 24, 1048–1064.

Elnashaie, S.S.E.H., Elshishini, S.S., 1993. Modelling. Simulation and Optimization of Industrial Fixed Bed Catalytic Reactors. Gordon and Breach Science Publishers, Switzerland.

EPA, 2003. National Primary Drinking Water Standards. EPA-816-F-03-016. Office of Water, June 2003, Washington, DC.

EPA, 2004. Potentiometric determination of nitrate in aqueous samples with ion-selective electrode. Method 9210. Test Methods for Evaluating Solid Waste, Physical/Chemical Methods, SW-846. Available on-line: <http://www.epa.gov/epaoswer/hazwaste/test/9_series.htm>.

Huang, Y.H., Zhang, T.C., 2004. Effects of low pH on nitrate reduction by iron powder. Water Res. 38, 2631–2642.

Huang, C.P., Wang, H.W., Chiu, P.C., 1998. Nitrate reduction by metallic iron. Water Res. 32, 2257–2264.

Kapoor, A., Viraraghavan, T., 1997. Nitrate removal from drinking water – review. J. Environ. Eng. – ASCE 123, 371–380.

Kim, H.H., Seagren, E.A., Davis, A.P., 2003. Engineered bioretention for removal of nitrate from stormwater runoff. Water Environ. Res. 75, 355–367.

Levenspiel, O., 1999. Chemical Reaction Engineering. John Wiley and Sons, Inc., New York.

Mishra, D., Farrell, J., 2005. Understanding nitrate reactions with zerovalent iron using Tafel analysis and electrochemical impedance spectroscopy. Environ. Sci. Technol. 39, 645–650.

Rocca, C.D., Belgiorno, V., Meriç, S., 2006. Overview of in-situ applicable nitrate removal processes. Desalination 204, 46–62.

Shuval, H.I., Gruener, N., 1977. Infant methemoglobinemia and other health effects of nitrates in dinking water. Prog. Water Technol. 8 (4–5), 183–193.

Sohn, K., Kang, S.W., Ahn, S., Woo, M., Yang, S.K., 2006. Fe(0) Nanoparticles for nitrate reduction: stability, reactivity and transformation. Environ. Sci. Technol. 40, 5514–5519.

Steinfeld, J.I., Francisco, J.S., Hase, W.L., 1989. Chemical Kinetics and Dynamics. Prentice-Hall, Inc., Englewood Cliffs, New Jersey.

Su, C., Puls, R.W., 2007. Removal of added nitrate in the single, binary, and ternary systems of cotton burr compost, zerovalent iron, and sediment: Implications for groundwater nitrate remediation using permeable reactive barriers. Chemosphere 67, 1653–1662.

Tamara, M.L., Butler, E.C., 2004. Effects of iron purity and groundwater characteristics on rates and products in the degradation of carbon tetrachloride by iron metal. Environ. Sci. Technol. 38, 1866–1876.

Yang, G.C.C., Lee, H.L., 2005. Chemical reduction of nitrate by nanosized iron: kinetics and pathways. Water Res. 39, 884–894.

Zawaideh, L.L., Zhang, T.C., 1998. The effects of pH and addition of an organic buffer (HEPES) on nitrate transformation in Fe^0-water systems. Water. Sci. Technol. 38 (7), 107–115.